Three-dimensional combined photoacoustic and optical coherence microscopy for *in vivo* microcirculation studies

Li Li[1], Konstantin Maslov[1], Geng Ku[1], Lihong V. Wang[1,*]

[1] *Optical Imaging Laboratory, Department of Biomedical Engineering, Washington University in St. Louis, 1 Brookings Drive, Campus Box 1097, St. Louis, Missouri 63130, USA*
*lhwang@biomed.wustl.edu

Abstract: Photoacoustic microscopy is predominantly sensitive to optical absorption, while optical coherence tomography relies on optical backscattering. Integrating their complementary contrasts can provide comprehensive information about biological tissue. We have developed a dual-modality microscope that combines the two for studying microcirculation. Three-dimensional imaging of microvasculature and its local environment has been demonstrated at micrometer-order resolution using endogenous contrast *in vivo*.

OCIS codes: (170.6900) Three-dimensional microscopy; (170.5120) Photoacoustic imaging; (170.4500) Optical coherence tomography; (170.1870) Dermatology; (170.4470) Ophthalmology.

References and links

1. H. F. Zhang, K. Maslov, G. Stoica, and L. V. Wang, "Functional photoacoustic microscopy for high-resolution and noninvasive *in vivo* imaging," Nat. Biotechnol. **24**(7), 848–851 (2006).
2. K. Maslov, H. F. Zhang, S. Hu, and L. V. Wang, "Optical-resolution photoacoustic microscopy for *in vivo* imaging of single capillaries," Opt. Lett. **33**(9), 929–931 (2008).
3. G. Ku, K. Maslov, L. Li, and L. V. Wang, "Photoacoustic microscopy with 2-μm transverse resolution," J. Biomed. Opt. under review.
4. L. V. Wang, "Tutorial on photoacoustic microscopy and computed tomography," IEEE J. Sel. Top. Quantum Electron. **14**(1), 171–179 (2008).
5. J. Oh, M. Li, H. F. Zhang, K. Maslov, G. Stoica, and L. V. Wang, "Three-dimensional imaging of skin melanoma *in vivo* by dual-wavelength photoacoustic microscopy," J. Biomed. Opt. **11**(3), 034032 (2006).
6. C. Vinegoni, T. Ralston, W. Tan, W. Luo, D. L. Marks, and S. A. Boppart, "Integrated structural and functional optical imaging combining spectral-domain optical coherence and multiphoton microscopy," Appl. Phys. Lett. **88**(5), 053901 (2006).
7. H. T. Chen, H. F. Wang, M. N. Slipchenko, Y. K. Jung, Y. Z. Shi, J. B. Zhu, K. K. Buhman, and J. X. Cheng, "A multimodal platform for nonlinear optical microscopy and microspectroscopy," Opt. Express **17**(3), 1282–1290 (2009), http://www.opticsinfobase.org/abstract.cfm?URI=oe-17-3-1282.
8. S. Y. Emelianov, S. R. Aglyamov, A. B. Karpiouk, S. Mallidi, S. Park, S. Sethuraman, J. Shah, R. W. Smalling, J. M. Rubin, and W. G. Scott, "Synergy and applications of combined ultrasound, elasticity, and photoacoustic imaging," 2006 IEEE Ultrasonics Symposium, 405–415 (2006).
9. J. J. Niederhauser, M. Jaeger, R. Lemor, P. Weber, and M. Frenz, "Combined ultrasound and optoacoustic system for real-time high-contrast vascular imaging *in vivo*," IEEE Trans. Med. Imaging **24**(4), 436–440 (2005).
10. B. Cense, N. A. Nassif, T. C. Chen, M. C. Pierce, S. H. Yun, B. H. Park, B. E. Bouma, G. J. Tearney, and J. F. de Boer, "Ultrahigh-resolution high-speed retinal imaging using spectral-domain optical coherence tomography," Opt. Express **12**(11), 2435–2447 (2004), http://www.opticsinfobase.org/oe/abstract.cfm?URI=oe-12-11-2435.
11. B. Fagrell, and M. Intaglietta, "Microcirculation: its significance in clinical and molecular medicine," J. Intern. Med. **241**(5), 349–362 (1997).
12. R. K. Jain, L. L. Munn, and D. Fukumura, "Dissecting tumour pathophysiology using intravital microscopy," Nat. Rev. Cancer **2**(4), 266–276 (2002).
13. R. G. Nadeau, W. Groner, J. W. Winkelman, A. G. Harris, C. Ince, G. J. Bouma, and K. Messmer, "Orthogonal polarization spectral imaging: a new method for study of the microcirculation," Nat. Med. **5**(10), 1209–1212 (1999).

14. J. Seylaz, R. Charbonné, K. Nanri, D. Von Euw, J. Borredon, K. Kacem, P. Méric, and E. Pinard, "Dynamic *in vivo* measurement of erythrocyte velocity and flow in capillaries and of microvessel diameter in the rat brain by confocal laser microscopy," J. Cereb. Blood Flow Metab. **19**(8), 863–870 (1999).
15. E. B. Brown, R. B. Campbell, Y. Tsuzuki, L. Xu, P. Carmeliet, D. Fukumura, and R. K. Jain, "*In vivo* measurement of gene expression, angiogenesis and physiological function in tumors using multiphoton laser scanning microscopy," Nat. Med. **7**(7), 864–868 (2001).
16. E. Eriksson, J. V. Boykin, and R. N. Pittman, "Method for *in vivo* microscopy of the cutaneous microcirculation of the hairless mouse ear," Microvasc. Res. **19**(3), 374–379 (1980).
17. H. F. Zhang, K. Maslov, and L. V. Wang, "*In vivo* imaging of subcutaneous structures using functional photoacoustic microscopy," Nat. Protocols **2**(4), 797–804 (2007).
18. J. Ai, and L. V. Wang, "Synchronous self-elimination of autocorrelation interference in Fourier-domain optical coherence tomography," Opt. Lett. **30**(21), 2939–2941 (2005).
19. European mutant mouse pathology database (Pathbase), "Scanning electron microscopy of the mouse ear," (University of Cambridge, 08/2009). http://eulep.pdn.cam.ac.uk/~skinbase/Anatomic_hair_types/EAR_ANNOTAT ED.jpg
20. H. F. Zhang, K. Maslov, M. Sivaramakrishnan, G. Stoica, and L. V. Wang, "Imaging of hemoglobin oxygen saturation variations in single vessels *in vivo* using photoacoustic microscopy," Appl. Phys. Lett. **90**(5), 053901 (2007).
21. Y. Zhao, Z. Chen, C. Saxer, S. Xiang, J. F. de Boer, and J. S. Nelson, "Phase-resolved optical coherence tomography and optical Doppler tomography for imaging blood flow in human skin with fast scanning speed and high velocity sensitivity," Opt. Lett. **25**(2), 114–116 (2000).
22. L. V. Wang, "Prospects of photoacoustic tomography," Med. Phys. **35**(12), 5758–5767 (2008).

As a fast emerging, noninvasive imaging tool, photoacoustic microscopy (PAM) [1–3] is currently capable of visualizing three-dimensional biological tissue *in vivo* at a resolution down to 2 µm. Compared to other optical microscopy technologies, PAM possesses a unique feature that it has a 100% relative sensitivity to optical absorption. A small fractional variation in the optical absorption coefficient causes the same amount of fractional change in the photoacoustic signal [4]. Many physiologically important molecules, e.g., hemoglobin and melanin, have strong characteristic optical absorption. As a result, PAM is especially appropriate for studying absorbing structures, such as blood micro-vessels [1–3] and melanoma [5]. However, without data about the surrounding tissues, the information carried in PAM images cannot be fully interpreted.

Recently, there exists an increasing trend in biomedical research to integrate multiple complementary microscopic imaging modalities into a single platform to provide comprehensive insights into physiology [6,7]. Previously, ultrasonic imaging has been suggested to complement photoacoustic imaging in deeper tissue [8,9]. However, it is difficult to resolve laterally beyond 10 µm while maintaining a reasonable penetration depth (~1 mm) in tissue using the ultrasonic method alone. In this letter, we demonstrate that a pure optical technique, optical coherence tomography (OCT), is a proper alternative. State-of-the-art OCT allows real-time, µm-resolution imaging of tissue up to a couple of millimeters deep *in vivo* [10]. The combination of PAM and OCT has several advantages. First, it provides completely complementary imaging contrasts. OCT exploits the scattering properties of tissue, while PAM is predominantly sensitive to optical absorption. Second, when designed properly, OCT and PAM can have comparable imaging depths and spatial resolutions, which are suitable for microscopic imaging.

A particularly useful application of the combined photoacoustic and optical-coherence microscopy is in studying microcirculation. Microcirculation is vital to sustain human health, and disturbed microcirculation is involved in most pathological processes [11]. Existing microscopic imaging techniques, although they have greatly facilitated our understanding of morphology, function and regulation of normal and pathological microcirculation, suffer from several limitations. Intravital microscopy [12] and orthogonal polarization spectral imaging [13] lack depth resolution, and thus are unable to show three-dimensional morphology of microvasculature. Confocal and multiphoton microscopy [14,15], although they can image tissue in three dimensions, generally require invasive introduction of exogenous fluorescence contrast agents. Our new tool overcomes these problems and is capable of noninvasively

imaging three-dimensional microvasculature and its local environment simultaneously, using only endogenous contrasts.

As the first demonstration of our dual-modality imaging strategy, we combined our optical-resolution PAM previously reported in [3] with spectral-domain OCT [10] in a single system. Figure 1 illustrates the experimental configuration of the dual-modality microscope. Both absorption- and scattering-contrast images were obtained from a unified platform, which resembled an inverted optical microscope. The object was illuminated from the bottom. The light used in both modalities was delivered to the platform through a single-mode optical fiber. The light coming out of the fiber tip was first shaped by an aspheric lens and then focused into the object by a microscope objective (Leica, E1, 4X/0.1). In both PAM and OCT images, the transverse resolution was determined by the optical focal size, and was estimated to be ~5 µm by imaging a USAF resolution target. During experiments, target objects were loaded on a cover slip using a custom-made holder, and were held stationary. The imaging platform was scanned using a fast two-dimensional precision linear stage. We were able to acquire x-z cross-sectional images across a 1-mm range within 0.4 seconds, which yielded a rate of 2.5 frames per second. A volumetric data set consisted of a series of x-z cross-sectional images taken at incremental y locations. A 2 µm lateral step size was typical for both PAM and OCT imaging.
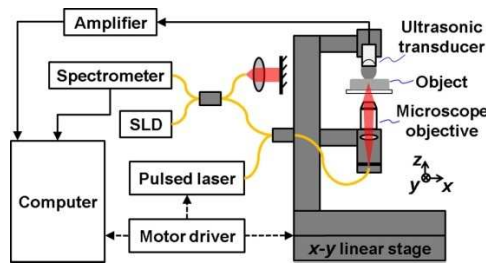

Fig. 1. Schematic of the combined photoacoustic and optical-coherence microscope. SLD: superluminescent diode. Solid lines represent single-mode optical fibers. Arrowhead solid lines show data flow. Arrowhead dashed lines show the flow of system control signals.

The PAM subsystem measures the time-resolved acoustic wave generated from laser-induced thermoelastic expansion of absorbing structures, such as blood vessels. It was irradiated by a diode-pumped Nd:YVO$_4$ laser (Elforlight, SPOT, 532 nm). Compared with other nanosecond-lasers currently used for photoacoustic imaging, this laser is compact, and can emit laser pulses as narrow as 1.2 ns at a pulse repetition rate as high as 20 KHz. To detect the generated photoacoustic wave, a spherically focused ultrasonic transducer (Olympus-NDT, V2022, center frequency: 75 MHz, focal length: 5 mm) was placed atop the object on the imaging platform. A drop of water was applied between the objective and the ultrasonic transducer for acoustic coupling. The photoacoustic axial resolution, mainly determined by the bandwidth of the ultrasonic detection, was estimated to be 14 µm [3]. At each transverse location, we collected the photoacoustic signal for 1 µs, which translated to an axial range of 1.5 mm.

The OCT subsystem measures the depth-resolved backscattered light from the object. It was configured as a fiber-based Michelson interferometer, and was seeded by a broadband superluminescent diode (InPhenix, IPSDD0803, λ_0 = 829 nm, $\Delta\lambda$ = 36.4 nm). The axial resolution, determined by the source bandwidth, was estimated to be 8.4 µm in air or 5.9 µm in soft tissue. The interference between the backscattered light from the object and a reference mirror was recorded by a homemade spectrometer. It was designed to have a spectral resolution of 67.5 pm, which limited the axial imaging range of OCT to 2.5 mm in air or 1.8 mm in tissue.

To demonstrate the capacity of our dual-modality microscope, we chose to image mouse ears, a long-established *in-vivo* animal model of cutaneous microcirculation that closely

resembles the human skin [16]. Because our microscope has a similar configuration to a traditional optical microscope, it can be readily applied to studying microcirculation *in vivo* using other popular animal models, such as a rodent dorsal skinfold chamber [12].We used nude mice (Harlan, 30g) in our experiments. During imaging, the mouse was anesthetized by a gas mixture of oxygen and 1% isoflurane at a flow rate of 1 L/min. After the experiments, all mice recovered naturally, and no visible photodamage was observed. All experimental procedures on animals conformed to the laboratory animal protocol approved by the School of Medicine Animal Studies Committee of Washington University in St. Louis. PAM and OCT images were obtained from raw data by following procedures described in Refs [17]. and [18], respectively.

Figure 2 shows that the *x-y* projectional images of a nude mouse ear obtained *in vivo* by our dual-modality microscope correlate well with the photograph taken through an optical microscope with 4X magnification. OCT and PAM visualized different aspects of the tissue better than the traditional optical microscope. In the OCT image (Fig. 2A), the sebaceous glands are resolved with higher resolution, due to the better rejection of background scattered light. The PAM image (Fig. 2B) clearly maps the microvasculature at higher contrast in greater details than the photograph. The average contrast-to-background ratio between blood micro-vessels and surrounding tissue was estimated to ~25:1, which manifests the advantage of the absorption-based photoacoustic method in imaging microvascular morphology. In Fig. 2C, we co-registered the two images, with the blood vessels in red and avascular structures in gray.
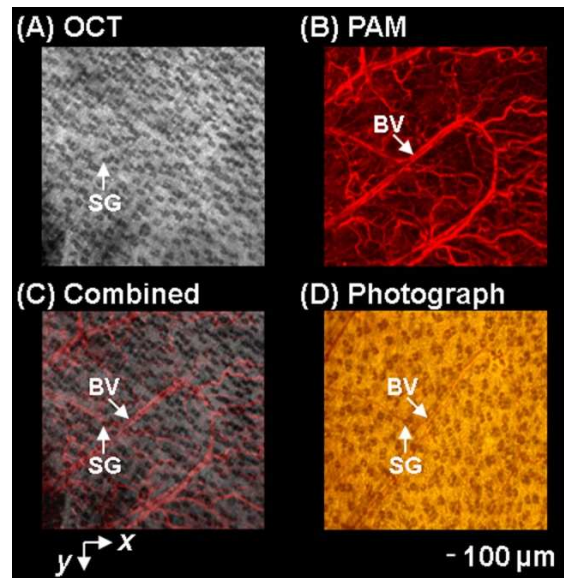

Fig. 2. *x-y* projection images of a nude mouse ear obtained by (A) OCT and (B) PAM. (C) Overlay of (A) and (B). (D) Photograph taken through an optical microscope. SG: sebaceous gland; BV: blood vessel.

The benefits of combining the complementary contrasts of OCT and PAM can be better appreciated by looking at a cross-section of tissue. To achieve axial resolution, PAM records the time-of-flight of sound, whereas OCT uses coherence gating. Figure 3 shows typical cross-sectional images of a nude mouse ear acquired by our microscope at a fixed *y* position, where the ventral side of the ear appears on the top. OCT provided us a microanatomy of the avascular structures in the ear (Fig. 3A). From the OCT cross-sectional images, we were able to estimate that the imaged regions had a thickness varying from 200 to 300 µm. Both OCT and PAM could see through them. By comparison with typical histology [19], we were able to

identify various structures in the ear. The ear consisted of two skin layers separated by a layer of non-scattering cartilage. The epidermis, the outmost layer of the skin, tended to be more scattering. The weak-scattering regions embedded in the skin layers were most likely sebaceous glands. We found more sebaceous glands in the dorsal skin layer than in the ventral layer, which agreed well with previous reports [16]. However, blood vessels were not evident on the OCT image. In contrast, PAM (Fig. 3B) is good at locating micro-vessels in the ear, with little information about the surrounding tissue forming the local environment of vessels. Some vessels, such as the one labeled as CP, had a diameter of ~7 µm, and were believed to be capillaries. From the co-registered cross-sectional image (Fig. 3C), we could identify the anatomical location of each imaged vessel. It was observed that the smallest vessels were located close to the skin surface. Other layers of vasculature were found near the cartilage layer. More interestingly, a large number of vessels were found to surround sebaceous glands, as reported earlier [16].
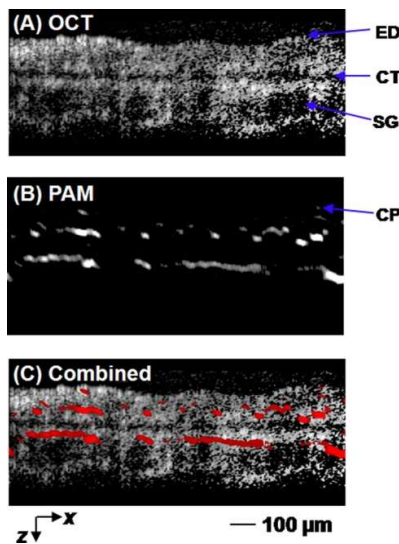

Fig. 3. *x-z* cross-sectional images of a mouse ear obtained by (A) OCT and (B) PAM. (C) Overlay of (A) and (B). ED, epidermis; CT, cartilage; SG, sebaceous gland; CP, capillary.

Both PAM and OCT are intrinsically three-dimensional imaging modalities. Neither PAM nor OCT requires scanning to resolve along the axial direction. In order to obtain a volumetric data set, our dual-modality microscope only needs two-dimensional raster scanning, unlike confocal and multi-photon microscopes, which depend on three-dimensional scanning. The three-dimensional PAM image (Fig. 4A) reveals details of the shape, direction, branching and connectivity of blood micro-vessels. Figure 4B shows a top view of the volumetric rendering of the dual-modality data set, where the microscopic epidermal ridges are evident from the OCT contrast. The distinguishable vascular morphologies in the ventral and dorsal layers of the skin are also compared in Figs. 4C and 4D.

We want to point out that PAM and OCT cannot only visualize structural relations between microvasculature and its local environment, but also quantify many important complementary hemodynamic functions. By exploiting the difference between the absorption spectra of oxy-hemoglobin and deoxy-hemoglobin, we can calculate the oxygen saturation (SO_2) and total concentration (THb) of hemoglobin locally in each single blood vessel using PAM images acquired with illumination at multiple wavelengths [20]. Moreover, OCT has been shown to be able to measure local blood flow as slow as 10 µm/s [21]. Currently, we are working to add these functional imaging capabilities to our dual-modality systems. By
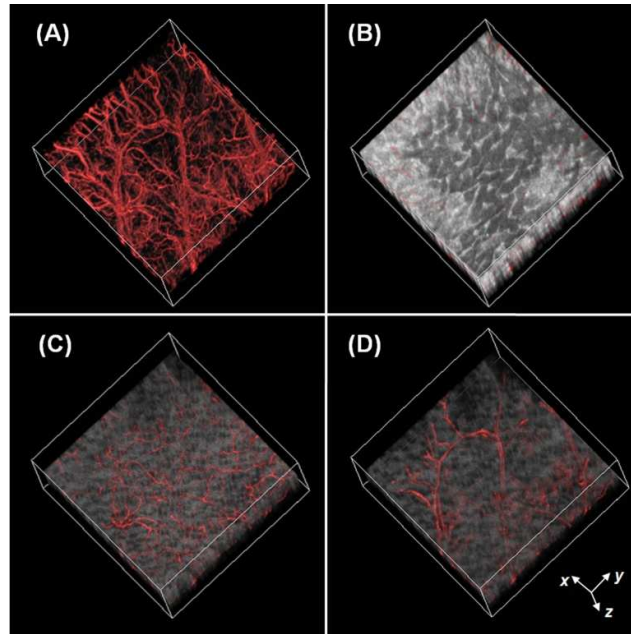
Fig. 4. 3D visualization of a mouse ear. (A) PAM image of the microvasculature only; (B) Dual-modality image showing the skin surface, a top view; (C) Dual-modality image showing the microvasculature in the ventral skin layer, a top view from 88 µm below the skin surface; (D) Dual-modality image showing the microvasculature in the dorsal skin layer, a top view from 148 µm below the skin surface. The bounding box has dimensions of 3.6 mm x 3.6 mm x 0.4 mm.

quantifying local SO_2, THb, and blood flow together, we expect to obtain additional functional indicators, such as the local oxygen metabolic rate, which may serve as a potential biomarker for diseases [22].

Last, it is also important to note that the presented microscope is just a paradigm of the strategy to combine photoacoustic imaging with optical coherence tomography. The concept itself is versatile in nature. The dual-modality microscopy can work fully in the reflection mode to allow access to various anatomical locations of interest by adopting alternative designs, for example using a light-ultrasound splitting component similar to the one used in Ref [2]. Also, its applications will not be limited to studying cutaneous microcirculation. With proper alternative designs, we expect that variant systems following the same concept can be potentially applied in studying other subjects, such as cerebral microcirculation and ophthalmological diseases.